Enhanced reactivity of nanoenergetic materials: A first-principles molecular dynamics study based on divide-and-conquer density functional theory

Fuyuki Shimojo,[1,2] Aiichiro Nakano,[1,a)] Rajiv K. Kalia,[1] and Priya Vashishta[1]
[1]*Department of Computer Science, Department of Physics and Astronomy, and Department of Chemical Engineering and Materials Science, Collaboratory for Advanced Computing and Simulations, University of Southern California, Los Angeles, California 90089-0242, USA*
[2]*Department of Physics, Kumamoto University, Kumamoto 860-8555, Japan*

(Received 27 May 2009; accepted 8 July 2009; published online 31 July 2009)

Integration of nanowires and nanoparticles of energetic materials into semiconducting structures is giving birth to "nanoenergetics-on-a-chip" technology. Understanding and controlling the reactions of nanoenergetic materials pose a theoretical challenge for combining quantum-mechanical accuracy with large scales to capture nanostructural effects. Recent developments in linear-scaling density functional theory have set a stage for first-principles molecular dynamics simulation of thermite reaction at an Al/Fe_2O_3 interface. Here, we report the finding of a concerted metal-oxygen flip mechanism that enhances mass diffusion and reaction rate at the interface. This mechanism leads to two-stage reactions, which may explain recent experimental observation in thermite nanowire arrays. © *2009 American Institute of Physics*. [DOI: 10.1063/1.3189143]

Recent advances in the integration of nanowires and nanoparticles of energetic materials into semiconducting electronic structures have opened up the possibility of "nanoenergetics-on-a-chip (NOC)" technology, which has a wide range of potential applications, such as micropropulsion in space and nanoairbags to drive nanofluidics.[1,2] Most widely used energetic materials for device integration are thermites, which are composites of metals and oxides. These materials have enormous energy release associated with the highly exothermic reduction/oxidation (redox) reactions to form more stable oxides. For example, arrays of Fe_2O_3 (Ref. 3) and CuO (Ref. 4) nanowires embedded in an Al matrix have been deposited on solid surfaces. Another example of thermite nanostructures is self-assembly of an ordered array of Al and Fe_2O_3 (Ref. 5) [or CuO (Ref. 6)] nanoparticles.

The integration of nanoenergetic materials into electronic circuits requires fundamental understanding and precise control of reaction rates and initiation time. The reactivity of nanoenergetic materials is known to differ drastically from their micron-scale counterparts. For example, experimental studies on the combustion of nanothermites, such as Al/Fe_2O_3 (Ref. 7) and Al/MoO_3,[8] have shown that flame propagation speeds approach km/s when the size of Al nanoparticles is reduced to below 100 nm, in contrast to cm/s for traditional thermites. Another example is the two-stage reaction of Al/CuO-nanowire thermite, in which the first reaction takes place at 500 °C followed by the second reaction at 660 °C (i.e., Al melting temperature).[4]

Such peculiar reactive behaviors of nanothermites cannot be explained by conventional mechanisms based on mass diffusion of reactants, and thus various alternative mechanisms have been proposed. An example is a mechanochemical mechanism that explains the fast flame propagation based on dispersion of the molten metal core of each nanoparticle and spallation of the oxide shell covering the metal core.[9] Another mechanism is accelerated mass transport of both oxygen and metal atoms due to the large pressure gradient between the metal core and the oxide shell of each metal nanoparticle.[10,11] In addition, defect-mediated giant diffusivity is important for fast reactions at the nanometer scale.[12–14]

The above mechanisms are by no means exhaustive, and some unexpected ones could operate in NOCs. It is therefore desirable to study the reaction of nanoenergetic materials by first-principles simulations. However, this poses an enormous theoretical challenge, where quantum-mechanical accuracy to describe chemical reactions must be combined with large spatial scales to capture nanostructural effects. Recent developments in linear-scaling density functional theory (DFT)[15–18] have set the stage for such large first-principles molecular dynamics (MD) simulation. We have performed divide-and-conquer DFT (DC-DFT) based MD simulations[15,18] to study the thermite reaction at an Al/Fe_2O_3 interface. The results reveal a concerted metal-oxygen flip mechanism that significantly enhances the rate of redox reactions. This mechanism leads to two-stage reactions—rapid initial reaction due to collective metal-oxygen flips followed by slower reaction based on uncorrelated diffusive motions, which may explain recent experimental observation in thermite nanowire arrays mentioned above.[4]

We simulate a stack of Al and Fe_2O_3 layers involving 1152 (144 Fe_2O_3+432 Al) atoms in an orthorhombic supercell with dimensions $(L_x, L_y, L_z) = (20.1, 26.2, 28.2$ Å) with periodic boundary conditions. The hematite (Fe_2O_3) crystal, cut along (0001) planes to expose Fe planes, is placed in the supercell with the (0001) direction parallel to the z direction. The Fe planes of the hematite are attached to (111) planes of the face-centered cubic Al crystal at the two interfaces. Our DC-DFT method[18] iteratively minimizes the energy functional using a preconditioned conjugate-gradient method[19,20] to determine electronic wave functions. The grid spacing ~0.25 Å (corresponding to the cutoff energy of 45 Ry in the plane-wave-based method) for the real-space representation of the wave functions is sufficiently small to obtain a

a)Electronic mail: anakano@usc.edu.

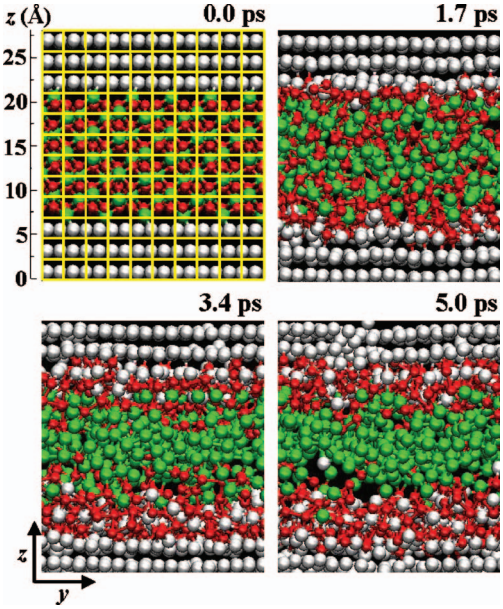

FIG. 1. (Color) Snapshots of the atomic configuration. The green, red, and gray spheres show the positions of Fe, O, and Al atoms, respectively. Yellow meshes at time 0 ps show the nonoverlapping cores used by the DC-DFT method. Two interfacial regions are defined as slabs with a thickness of 4 Å parallel to the *xy* plane (length scale in angstrom is marked in the *z* direction). The Al- and Fe-side regions are defined between the two interfacial regions.

good convergence of the total energy. We use a norm-conserving pseudopotentials[21] and a generalized gradient approximation[22] for the exchange-correlation energy. The DC-DFT method divides the system into 960 ($=8\times10\times12$) domains of dimensions $2.51\times2.62\times2.35$ Å^3. Figure 1 shows the side (*yz*) view of the nonoverlapping cores of the domains in the supercell. Each domain is augmented with a buffer layer of depth ~2.2 Å to avoid boundary effects. The interatomic forces thus computed quantum mechanically are used to integrate Newton's equations of motion numerically (with a time step of 0.84 fs) in MD simulations to study atomic motions and chemical reactions. The MD simulations are carried out at temperature 2000 K in the canonical ensemble. The simulation for 5 ps (6000 MD time steps) took 985 h on 960 (3.2 GHz Intel Xeon) processors.

Snapshots of the atomic configuration are shown in Fig. 1, where the side (*yz*) views of atomic configuration are displayed. We observe that the oxygen atoms in hematite migrate into the aluminum metal to form aluminum oxide and leaves behind liquid iron. Our DC-DFT simulation thus describes complete thermite reaction, $2Al+Fe_2O_3\rightarrow Al_2O_3+2Fe$.

To study mass diffusivity, Fig. 2 shows mean square displacements of O atoms along the *z* direction, which are calculated using the simulation data for 0–3 ps. The solid and dashed lines are obtained from O atoms in the interfacial and Fe-side regions, respectively. Here, the boundary between iron oxide and aluminum oxide at each interface is located by calculating the average *z* coordinate of Al atoms facing Fe atoms. The interfacial regions are then defined as slabs with a thickness of 4 Å (i.e., 2 Å above and below the boundaries) parallel to the *xy* plane as shown in Fig. 1. Figure 2 shows that O atoms in the interfacial region are much more diffusive than those on the Fe side. The fourfold accelerated diffusion constant perpendicular to the interface is 2×10^{-4} cm^2/s in the interfacial region.

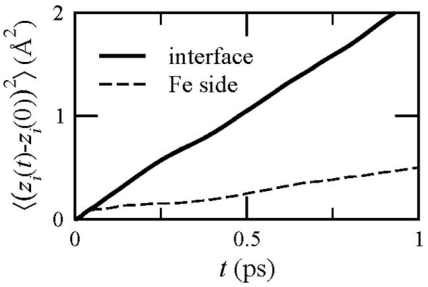

FIG. 2. Enhanced diffusion at the metal-oxide interface. Mean square displacements of O atoms along the *z* direction are plotted as a function of time. The solid and dashed curves are for O atoms in the interfacial and Fe-side regions, respectively.

To understand the mechanism of the enhanced diffusivity at the interface, we have examined the time evolution of the atomic configuration in the interfacial region and found a concerted metal-oxygen flip mechanism. That is, O atoms switch their positions with neighboring Al atoms while diffusing in the *z* direction. A typical example of such events is shown in Fig. 3, where the middle panel shows the time evolution of the *z* coordinates of the O and Al atoms of interest. The O atom moves upward in concert with the Al atom moving downward. The switching motion between the O and Al atoms is shown in the bottom panel of Fig. 3.

To explain the quantum-mechanical origin of this mechanism, we calculate the bond-overlap population $O_{ij}(t)$ between *i*th and *j*th atoms as a function of time *t*.[23] We also define the sum of the bond-overlap population (SBOP) for each oxygen atom. Partial SBOP $O_i^\alpha(t)$ for the *i*th oxygen atom is defined as $O_i^\alpha(t)=\Sigma_{j\in\alpha}O_{ij}(t)$, where α is Fe or Al, and the total SBOP is $O_i(t)=O_i^{Fe}(t)+O_i^{Al}(t)$. The upper panel

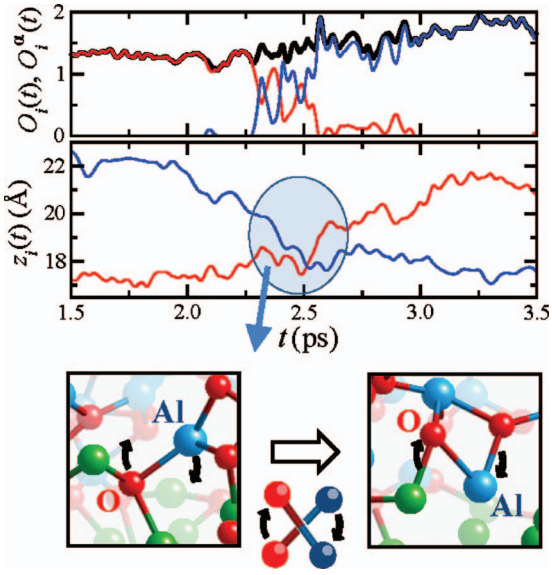

FIG. 3. (Color) Concerted metal-oxygen flip mechanism. (Top panel) Time evolution of the total and partial SBOP, $O_i(t)$ and $O_i^\alpha(t)$, associated with the oxygen atom labeled as "O" in the bottom panel. The black, red, and blue curves show $O_i(t)$, $O_i^{Fe}(t)$, and $O_i^{Al}(t)$, respectively. (Middle panel) Time evolution of the *z* coordinates of the O and Al atoms labeled as O and 'Al' in the bottom panel, respectively. (Bottom panel) Atomic configurations near the O and Al atoms of interest (labeled as O and Al) at 2.3 and 2.8 ps. The green, red, and blue spheres are Fe, O, and Al atoms, respectively.

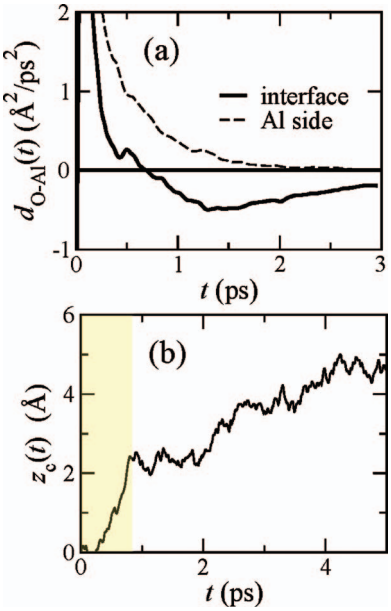

FIG. 4. (Color) (a) Negative correlation associated with concerted Al and O motions at the interface. Correlation functions between displacements of O and Al atoms along the z direction [defined in Eq. (1)] are shown as a function of time. The solid and dashed curves are obtained in the interfacial and Al-side regions. (b) Two-stage reactions of thermite. Time evolution of the positions $z_c(t)$ of the reaction fronts. The yellow shade highlights the rapid first-stage reaction due to concerted Al–O motions, which is followed by slow reaction based on uncorrelated diffusion.

of Fig. 3 shows $O_i(t)$ and $O_i^{\alpha}(t)$ associated with the O atom. For $t<2.3$ ps, the oxygen atom resides in the iron-oxide region, and $O_i^{Fe}(t)$ has finite values, while $O_i^{Al}(t)$ is nearly zero. At $t\sim 2.3$ ps, the oxygen atom starts to migrate into the aluminum side and $O_i^{Al}(t)$ begins to increase. For 2.3 ps$<t<$2.7 ps, $O_i^{Fe}(t)$ and $O_i^{Al}(t)$ have comparable values while the oxygen atom is moving across the interface. For $t>3.0$ ps, $O_i^{Fe}(t)$ becomes zero, while $O_i^{Al}(t)$ converges to a finite value, indicating that the oxygen atom is chemically bonded only with Al atoms. The switching motion between O and Al atoms at the interface is thus triggered by the change of chemical bonding associated with these atoms.

To quantify the collective switching motion between O and Al atoms, we calculate the correlation function between the displacements of atoms along the z direction:

$$d_{O-Al}(t) = \langle \Delta z_i(t) \cdot \Delta z_j(t) \rangle / t^2, \quad (1)$$

where $\Delta z_i(t)=z_i(t+t_0)-z_i(t_0)$ with $z_i(t)$ being the z coordinate of the ith ion at time t. The brackets mean the average over both the time origin t_0 and atomic pairs ($i\in O, j\in Al$). In the calculation, atomic pairs whose distance is less than 2.3 Å at t_0 are selected. Since we are interested in the correlation between diffusing O and Al atoms, we include atomic pairs that satisfy the conditions $|\Delta z_i(t)|>2$ Å and $|\Delta z_j(t)|>2$ Å at $t=2$ ps. The results in Fig. 4(a) (solid curve) reveal negative correlation in $d_{O-Al}(t)$ for $t>0.5$ ps, which reflects the collective switching motion between O and Al atoms at the interface as shown in Fig. 3. Such negative correlation does not exist on the Al side [see the dashed curve in Fig. 4(a)], indicating independent diffusive motions of Al and O atoms.

The enhanced mass diffusivity at the metal-oxide interface leads to a two-stage reaction behavior. In Fig. 4(b), we plot the position $z_c(t)$ of the reaction front calculated from the coordinates of oxygen atoms at the forefront of oxidation. For $t<1$ ps, $z_c(t)$ increases rapidly as oxygen atoms migrate into the Al side, which is accelerated by the collective switching mechanism. This is followed by a slower reaction due to uncorrelated diffusion of atoms. (Though slower than the concerted thermite reaction, the second-stage diffusion here could still be faster than conventional diffusion due to defect-mediated giant diffusivity[12–14] because of the depletion of O atoms in the near-interface oxides.) Such two-stage reactions may be related to the experimental observation in thermite nanowire arrays mentioned before.[4]

In summary, our large first-principles MD simulation based on DC-DFT reveals a concerted metal-oxygen flip mechanism that significantly enhances mass diffusivity and the rate of thermite reactions at an Al/Fe_2O_3 interface.

This work was partially supported by ARO-MURI (W911NF-04-1-0178), and DTRA (HDTRA1-07-1-0023). F.S. acknowledges support by Grant-in-Aid for Scientific Research on Priority Area, "Nanoionics (439)" from the MEXT, Japan. Simulations were performed at the Collaboratory for Advanced Computing and Simulations. We thank Professor Richard Yetter and Dr. Suhithi Peiris for stimulating discussions.

[1] C. Rossi and D. Esteve, Sens. Actuators, A **120**, 297 (2005).
[2] C. Rossi, K. Zhang, D. Esteve, P. Alphonse, P. Tailhades, and C. Vahlas, J. Microelectromech. Syst. **16**, 919 (2007).
[3] L. Menon, S. Patibandla, K. B. Ram, S. I. Shkuratov, D. Aurongzeb, M. Holtz, J. Berg, J. Yun, and H. Temkin, Appl. Phys. Lett. **84**, 4735 (2004).
[4] K. Zhang, C. Rossi, G. A. A. Rodriguez, C. Tenailleau, and P. Alphonse, Appl. Phys. Lett. **91**, 113117 (2007).
[5] S. H. Kim and M. R. Zachariah, Adv. Mater. (Weinheim, Ger.) **16**, 1821 (2004).
[6] J. Y. Malchi, Ph.D. thesis, The Pennsylvania State University, 2007.
[7] K. B. Plantier, M. L. Pantoya, and A. E. Gash, Combust. Flame **140**, 299 (2005).
[8] B. S. Bockmon, M. L. Pantoya, S. F. Son, B. W. Asay, and J. T. Mang, J. Appl. Phys. **98**, 064903 (2005).
[9] V. I. Levitas, B. W. Asay, S. F. Son, and M. Pantoya, Appl. Phys. Lett. **89**, 071909 (2006).
[10] T. J. Campbell, R. K. Kalia, A. Nakano, P. Vashishta, S. Ogata, and S. Rodgers, Phys. Rev. Lett. **82**, 4866 (1999).
[11] A. Rai, K. Park, L. Zhou, and M. R. Zachariah, Combust. Theory Modell. **10**, 843 (2006).
[12] N. N. Thadhani, J. Appl. Phys. **76**, 2129 (1994).
[13] Y. Chen, Z. Lu, K. Nomura, W. Wang, R. K. Kalia, A. Nakano, and P. Vashishta, Phys. Rev. Lett. **99**, 155506 (2007).
[14] M. Legros, G. Dehm, E. Arzt, and T. J. Balk, Science **319**, 1646 (2008).
[15] W. T. Yang, Phys. Rev. Lett. **66**, 1438 (1991).
[16] S. Goedecker, Rev. Mod. Phys. **71**, 1085 (1999).
[17] D. R. Bowler, J. L. Fattebert, M. J. Gillan, P. D. Haynes, and C. K. Skylaris, J. Phys.: Condens. Matter **20**, 290301 (2008).
[18] F. Shimojo, R. K. Kalia, A. Nakano, and P. Vashishta, Phys. Rev. B **77**, 085103 (2008).
[19] G. Kresse and J. Furthmuller, Phys. Rev. B **54**, 11169 (1996).
[20] F. Shimojo, R. K. Kalia, A. Nakano, and P. Vashishta, Comput. Phys. Commun. **140**, 303 (2001).
[21] N. Troullier and J. L. Martins, Phys. Rev. B **43**, 8861 (1991).
[22] J. P. Perdew, K. Burke, and M. Ernzerhof, Phys. Rev. Lett. **77**, 3865 (1996).
[23] N. Umezawa, R. K. Kalia, A. Nakano, P. Vashista, and F. Shimojo, J. Chem. Phys. **126**, 234702 (2007).